Support Information

Third-order optical nonlinearities of zinc porphyrins accommodated in the cavity of doughnut-like molybdenum crown cluster

Ran Sun, Ting Wang, Xiaoyu Ren, Lijuan Zhang,* Yunshan Zhou* and Chengcheng Huang

State Key Laboratory of Chemical Resource Engineering, College of Chemistry, Beijing University of Chemical Technology, Beijing 100029, P. R. China

Synthesis of 5,10,15,20-Tetracarboxylic Tetraphenyl Zinc Porphyrin (ZnTCPP)

ZnTCPP was synthesized according to the reported method [1]. Main infrared spectral data (KBr, cm^{-1}): 3417 (w), 1682 (s), 1595 (s), 1387 (m), 1259 (w), 1103 (w), 989 (s), 785 (w). ^1H NMR (400 MHz, DMSO-d_6): δ 13.31 (s, 4 H), 8.80 (d, J = 1.4 Hz, 8 H), 8.36 (d, J = 1.0 Hz, 8 H), 8.30 (d, J = 7.9 Hz, 8 H). [2]

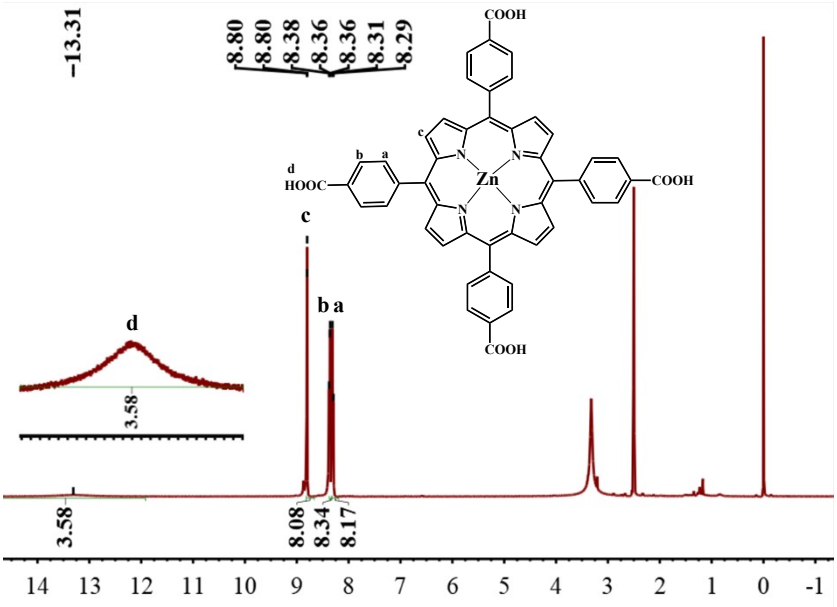

Fig. S1 The ^1H-NMR spectrum of ZnTCPP in DMSO-d_6.

Synthesis of 5,10,15, 20-Tetrahydroxy Tetraphenyl Zinc Porphyrin (ZnTHPP)

ZnTHPP was synthesized according to the reported method. [3] Main infrared spectral data (KBr, cm^{-1}): 1541 (s), 1458 (m), 1327 (w), 1255 (m), 1159 (m), 991 (s), 800 (s). ^1H NMR (400 MHz, DMSO-d_6): δ 9.83 (s, 4 H), 8.80 (s, 8 H), 7.95 (d, J = 8.4 Hz, 8 H), 7.17 (d, J = 8.4 Hz, 8 H).

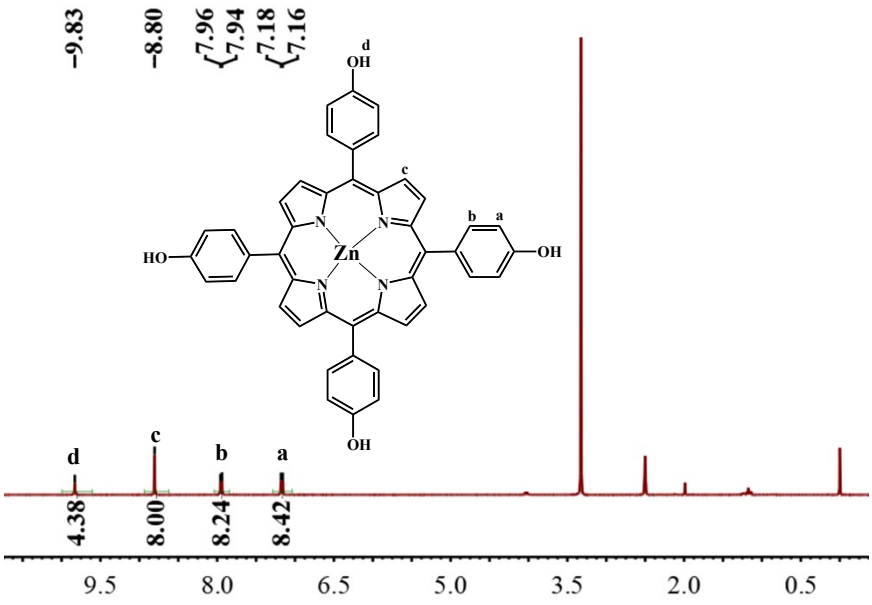

Fig. S2 The ^{1}H-NMR spectrum of ZnTHPP in DMSO-d_6.

Synthesis of 5,10,15,20-Tetramino Tetraphenyl Zinc Porphyrin (ZnTAPP)

ZnTAPP was synthesized according to the reported method [5]. Main infrared spectral data (KBr, cm^{-1}): 3390(s), 1653 (s), 1608 (w), 1466 (w), 1168 (s), 989 (w), 796 (w). ^{1}H NMR (400 MHz, DMSO-d_6): δ 8.83 (S, 8 H), 7.81 (D, J = 8.1 Hz, 8 H), 6.98 (D, J = 8.1 Hz, 8 H), 5.44 (S, 8 H).

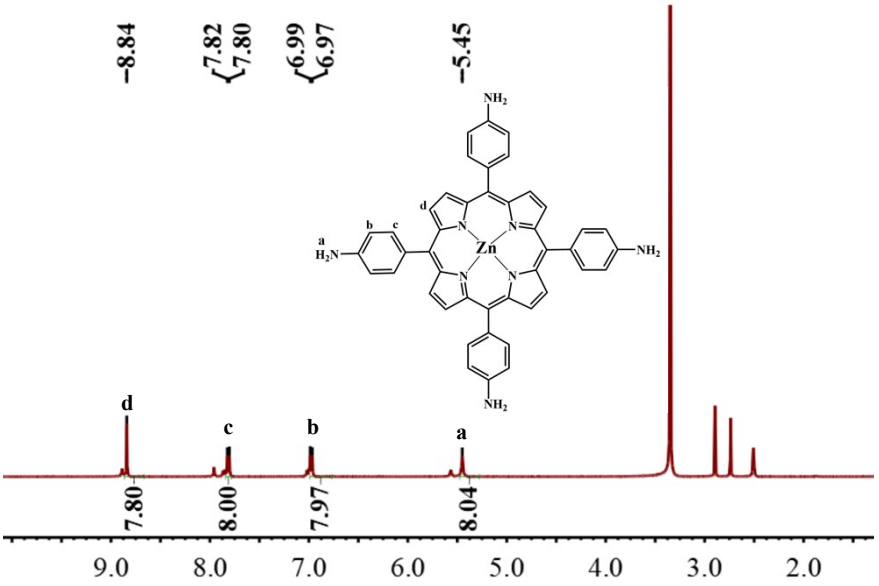

Fig. S3 The ^{1}H-NMR spectrum of ZnTAPP in DMSO-d_6.

Synthesis of $Na_{16}[(MoO_3)_{176}(H_2O)_{63}(CH_3OH)_{17}H_{16}]\cdot ca.100H_2O$

{Mo_{176}} was synthesized according to the literature [7]: 7.3 mL 25%

hydrochloric acid solution and 30 mL methanol solution were slowly added into 60 mL 0.5 mol/L $Na_2MoO_4 \cdot 2H_2O$ (7.26 g, 30.01 mmol) aqueous solution. Hydrazine hydrochloride (0.14 g, 1.30 mmol) was then added to the above solution, stirred for 5 minutes and sealed for 7 days, obtaining a large amount of dark blue powder. The dark blue powder $\{Mo_{176}\}$ was collected by filtered dark blue solid, washed quickly with a small amount of ice water and vacuum dried at 85 ℃. (4.81 g, 95.3%). Main infrared spectral data (KBr, cm^{-1}): 1610 (w), 1383 (w), 1036 (s), 964 (s), 746 (m), 559 (s).

Z-scan measurement[8]

As shown in Fig. S4, the Z-scan device consists of two laser energy detectors, D_1 and D_2, which respectively detect the intensity of the incident light after the laser passes through the spectroscope and the intensity of the outgoing light after the laser passes through the sample. The sample moves along the Z-axis during the whole test process, and the detector can record the incident light intensity and outgoing light intensity of the sample at different positions. The transmittance curve of the sample can be obtained by analyzing these data. When the test moves from -z to +z, the curve detected by D_2 detector is an open hole curve. The sample at the focus has the strongest nonlinear absorption effect and all data are symmetric about the focus. When the transmittance image shows the peak, the sample is saturated absorption, $\beta > 0$; when the transmittance image shows a valley value, the sample is anti-saturated absorption, $\beta < 0$[9]. As the test moves from + z to - z, the D_2 detector detects a closed-cell curve, and the nonlinear refraction of the sample is affected by position.When the transmittance image is peak-to-valley, the nonlinear refractive index coefficient is negative, and the sample is self-defocusing refraction. When the transmittance image presents the form of first valley and then peak, the nonlinear refractive index coefficient is positive, and the sample shows self-focusing refraction[10]. In this chapter, the third order NLO parameter is discussed to judge whether hybrid materials are a class of nonlinear optical materials with research value.

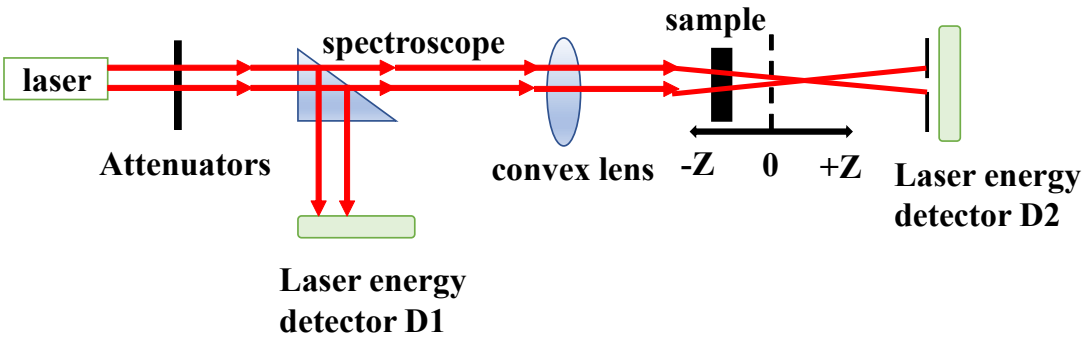

Fig. S4 The schematic diagram of Z-scan test instrument.

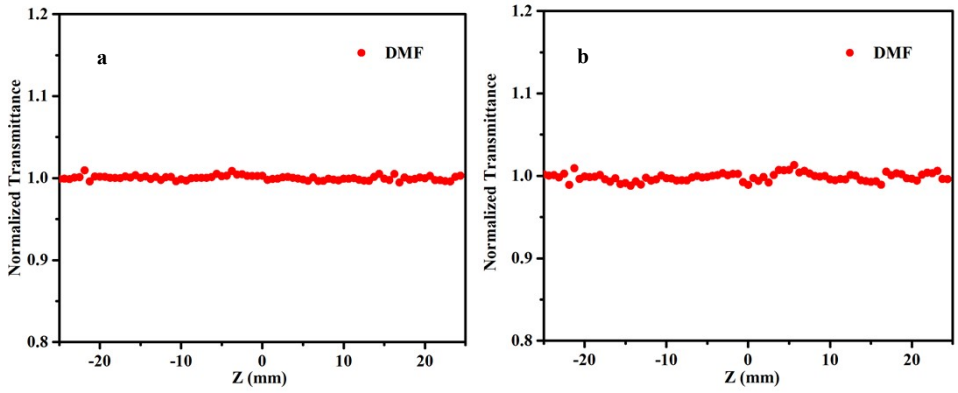

Fig. S5 The Z-Scan curves of DMF (a: open-aperture curves; b: closed-aperture curves)

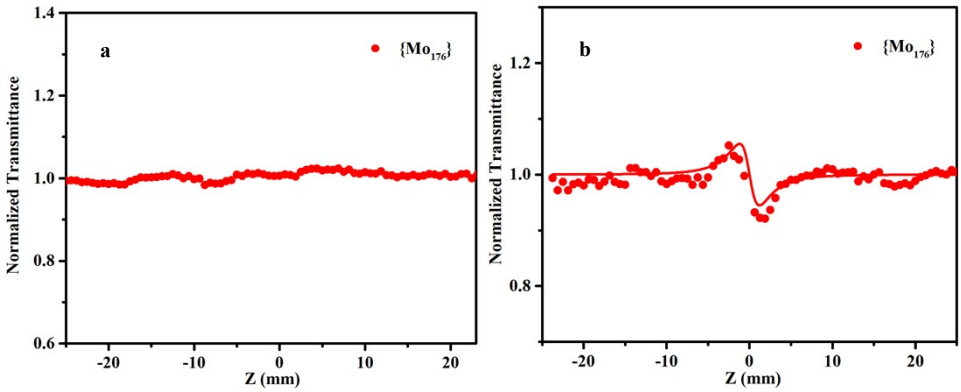

Fig. S6 The Z-Scan curves of $\{Mo_{176}\}$ (a: open-aperture curves; b: closed-aperture curves; solvent: water; c = 1.0×10^{-5} mol/L)

Table S1 The third NLO parameters of different compounds.

Compounds	β value (esu)	Test condition	Ref.
$CH_3NH_3PbB_3$	$(8.6 \pm 0.5) \times 10^{-6}$	λ = 800 nm; τ = 100 fs	11

Anderson type-TPP	48.7×10^{-6}	$\lambda = 532$ nm, $\tau = 6$ ns	12
GO	2.5×10^{-9}	$\tau = 4$ ns; $\lambda = 532$ nm	13
$tBu_4PcGaCl$/PMMA	8.96×10^{-6}	$\lambda = 532$ nm; $\tau = 6$ ns	14

Table S2 The limiting thresholds of different OL materials.

Compound	Limiting Threshold (J/cm^2)	Ref.
1	0.30	our work
MoS_2	11.16	15
Graphene	15.15	15
phthalocyaninato-triazin	0.79	16
ZnTPyP-1/PDMS	0.58	17
LPB–30	0.54	18
N-CD-Pt	0.62	19
Sn-Pc-POF	0.37	20

Reference

1. D. W. Feng, Z. Y. Gu, J. R. Li, H. L. Jiang, Z. W. Wei and H. C. Zhou, *Angew. Chem. Int. Edit.*, 2012, **51**, 10307-10310.
2. Y. Z. Wang, J. Sun, H. H. Zhang, Z. P. Zhao and W. F. Liu, *Catal. Sci. Technol.*, 2018, **8**, 2578-2587.
3. V. D. Rumyantseva, A. S. Gorshkova and A. F. Mironov, *Macroheterocycles*, 2013, **6**, 59-61.
4. R. Shen, W. Zhu, X. D. Yan, T. Li, Y. Liu, Y. X. Li, S. Y. Dai and Z. G. Gu, *Chem. Commun.*, 2019, **55**, 822-825.
5. W. J. Meng, B. Breiner, K. Rissanen, J. D. Thoburn, J. K. Clegg and J. R. Nitschke, *Angew. Chem. Int. Edit.*, 2011, **50**, 3479-3483.
6. S. S. Q. N. Muller A., Bogge H., Schmidtmann M., *Nature*, 1999, **397**, 48-50.
7. A.MuÈller, C. Beugholt, M. Koop, K. D. Samar, S. Marc and H. Bogge, *Z. Anorg. Allg. Chem.*, 1999, **625**, 1960-1962.
8. G. R. A. D. Maria, A. L. Fernando, *Proc. Spie.*, 1998, **3473**, 91-100.
9. Z. H. Shi, Y. S. Zhou, L. J. Zhang, S. Hassan and N. N. Qu, *J. Phys. Chem. C*, 2014, **118**, 6413-6422.
10. M. B., B. R. and S. G., *Journal of Materials Science: Materials in Electronics*, 2017, **28**, 13740-13749.
11. G. Walters, B. R. Sutherland, S. Hoogland, D. Shi, R. Comin, D. P. Sellan, O. M. Bak and E. H. Sargent, *ACS Nano*, 2015, **9**, 9340–9346.
12. S. Hassan, H. M. Asif, Y. S. Zhou, L. J. Zhang, N. N. Qu, J. Q. Li and Z. H. Shi, *J. Phys. Chem.*

C, 2016, **120**, 27587-27599.
13. I. Papadakis, A. Bakandritsos, A. K. Swain, T. Szabo and S. Couris, *J. Phys. Chem. C*, 2020, **124**, 11265-11273.
14. Y. Chen, N. He, J. J. Doyle, Y. Liu, X. D. Zhuang and W. J. Blaub, *J. Photoch. Photobio. A*, 2007, **189**, 414-417.
15. D. N., L. Y., F. Y., Z. S., Z. X., C. C., F. J., Z. L. and W. J., *Scientific Reports*, 2015, **5**, 14646.
16. S. K. E., A. Edith and N. Tebello, *Polyhedron*, 2015, **85**, 347-354.
17. L. D. J., L. Q. H., W. Z. R., M. Z. Z., G. Z. G. and Z. J., *Journal of the American Chemical Society*, 2021, **143**, 17162-17169.
18. J. G., G. A., R. S. V., A. D. A., K. G. M., G. M., D. K. K., F. J. M. F. and A. A. R., *Scripta Materialia*, 2022, **211**.
19. Z. S. Q., Z. Q., P. Q. Q., H. J. Y., L. R., S. G. L. and Z. H. J., *Applied Surface Science*, 2022, **584**.
20. W. T. F., S. T., T. W., H. W. B., Z. W. X., Y. L. H., S. J. H. and M. H. P., *New Journal of Chemistry*, 2020, **44**, 15345-15349.